JOURNAL OF MORPHOLOGY 276:1377–1391 (2015)

Linking Cranial Morphology to Prey Capture Kinematics in Three Cleaner Wrasses: *Labroides dimidiatus*, *Larabicus quadrilineatus*, and *Thalassoma lutescens*

Vikram B. Baliga* and Rita S. Mehta

Department of Ecology and Evolutionary Biology, Long Marine Laboratory, University of California Santa Cruz, Santa Cruz, California 95060

ABSTRACT Cleaner fishes are well known for removing and consuming ectoparasites off other taxa. Observers have noted that cleaners continuously "pick" ectoparasites from the bodies of their respective client organisms, but little is known about the kinematics of cleaning. While a recent study described the jaw morphology of cleaners as having small jaw-closing muscles and weak bite forces, it is unknown how these traits translate into jaw movements during feeding to capture and remove ectoparasites embedded in their clients. Here, we describe cranial morphology and kinematic patterns of feeding for three species of cleaner wrasses. Through high-speed videography of cleaner fishes feeding in two experimental treatments, we document prey capture kinematic profiles for *Labroides dimidiatus*, *Larabicus quadrilineatus*, and *Thalassoma lutescens*. Our results indicate that cleaning in labrids may be associated with the ability to perform low-displacement, fast jaw movements that allow for rapid and multiple gape cycles on individually targeted items. Finally, while the feeding kinematics of cleaners show notable similarities to those of "picker" cyprinodontiforms, we find key differences in the timing of events. In fact, cleaners generally seem to be able to capture prey twice as fast as cyprinodontiforms. We thus suggest that the kinematic patterns exhibited by cleaners are indicative of picking behavior, but that "pickers" may be more kinematically diverse than previously thought. J. Morphol. 276:1377–1391, 2015.

KEY WORDS: cleaner fish; kinematics; morphology; cleaning behavior; picking

INTRODUCTION

In fishes, cleaning behavior is a mutualistic service that involves the consumption of ectoparasites off other taxa. Over 120 species of teleost fishes exhibit cleaning behavior, and cleaners are spread across 18 marine families (Côté, 2000; Froese and Pauly, 2015). The majority of cleaner fishes (at least 75 species) exhibit cleaning behavior predominately as juveniles, transitioning from this feeding strategy over ontogeny (Côté, 2000; Froese and Pauly, 2015).

Why certain species clean as juveniles while others do not is poorly understood. A recent study that examined cleaners and non-cleaning close relatives revealed that as juveniles, cleaners possess weak jaws with low mobility, among other traits. As cleaner fishes grow, they show positive allometry for many traits functionally related to feeding, which may facilitate transitions away from cleaning into adulthood (Baliga and Mehta, 2014).

How distinct the prey capture kinematics of cleaning are from other well-documented prey capture behaviors in fishes is not clear. We predict cleaners to possess not only morphological adaptations, but also specialized jaw movements during feeding to capture and remove ectoparasites embedded in their clients. Workers have informally described cleaners as continuously "picking" ectoparasites from the bodies of their respective client organisms (Darcy et al., 1974; Losey et al., 1994). The functional morphology of cleaning, however, has not been systematically studied, and kinematic details of prey acquisition have yet to be uncovered.

Others have used the term "picking" to describe a form of manipulation in some cichlids (Liem, 1979), or a form of prey capture by biting in embiotocids and labrids (Horn and Ferry-Graham, 2006). Here, a predator's precise and repeated movements of its upper jaws allow protruding teeth to be used as a prehensile tool used to dislodge small, sessile prey from a substrate (Liem,

Additional supporting information may be found in the online version of this article.

*Correspondence to: Vikram B. Baliga; 150B Center for Ocean Health, Long Marine Laboratory, Santa Cruz, CA 95060.
E-mail: vbaliga@ucsc.edu

Conflict of Interest: The authors have no conflicts of interest to declare.

Received 6 March 2015; Revised 3 June 2015;
Accepted 11 July 2015.

Published online 12 August 2015 in
Wiley Online Library (wileyonlinelibrary.com).
DOI 10.1002/jmor.20425

1979). In Cyprinodontiformes, "picking" is also used to describe precisely controlled and coordinated "forceps-like" movements of the upper and lower jaws (Ferry-Graham et al., 2008; Hernandez et al., 2009). In contrast to other forms of biting, cyprinodontiform picking involves the selective acquisition of individual prey items (small invertebrate prey) from the substrate or water column, while other items are left behind (Hernandez et al., 2008). The fine-tuned precise movements underlying the picking behavior in cyprinodontiform taxa are associated with a morphological novelty in the premaxillomandibular ligament connecting the upper and lower jaws (Hernandez et al., 2008).

Whether picking in cleaner fishes is similar to the picking behavior observed in other taxa is unknown and can only be determined through kinematic studies. We hypothesize that cleaner fishes employ a similar feeding strategy, using precise, coordinated movements of the jaws, leading to the removal of targeted items from a client's body while leaving little room for error in haphazardly biting into the client itself. Whether morphological novelties have evolved in association with cleaning has not been determined.

The mostly coral reef-associated clade Labridae (wrasses and parrotfishes) contains more known cleaner fish species than in any other group (Côté, 2000; Froese and Pauly, 2015). We report on the cranial morphology and kinematic patterns of feeding of three labrids: *Labroides dimidiatus* (Valenciennes, 1839), *Larabicus quadrilineatus* (Rüppell, 1835), and *Thalassoma lutescens* (Lay and Bennet, 1839). Of these three species, only *L. dimidiatus* is described as an obligate cleaner fish; it is known to clean throughout ontogeny, and obtains >85% of its dietary items through cleaning (Côté, 2000). The monotypic *L. quadrilineatus* is a close relative of *L. dimidiatus*; as shown in Cowman and Bellwood (2011), this species is immediately sister to the monophyletic group containing all the *Labroides* taxa. Unlike its close relatives in *Labroides*, *Larabicus* is reported to be a facultative (juvenile) cleaner (Côté, 2000), and has been shown to undergo an ontogenetic transition away from cleaning as it enters adulthood (Randall and Springer, 1975; Randall, 1986). The size at which this shift occurs is not precisely known. Cole (2010) found that in the closely related *Diproctacanthus xanthurus* and *Labropsis alleni*, a precipitous decrease in cleaning occurs when these species reach approximately 35 and 45 mm standard length, respectively. Given that *Larabicus, Diproctacanthus*, and *Labropsis* all transition away from cleaning to obligate corallivory in adulthood, and each attains a similar maximum adult size, it is reasonable to assume that the transition away from cleaning also occurs around 35–45 mm standard length in *Larabicus*. Similarly, *T. lutescens* is a facultative (juvenile) cleaner (Côté, 2000). This species is more distantly related to the other taxa in this study, and is one of several *Thalassoma* species that cleans facultatively (Côté, 2000; Baliga and Mehta, 2014). *T. lutescens* exhibits a dietary shift away from cleaning as it enters adulthood (McCourt, 1984), which was recently found to be at approximately 85-mm standard length (Baliga and Mehta, 2014).

While the cranial morphology of the obligate cleaner *L. dimidiatus* has been described previously (Tedman, 1980a,b), a more generalized view of cleaner fish morphology is lacking. Furthermore, it has not been established how the morphology of cleaner fishes relates to the kinematic patterns they exhibit. Our goals were thus to 1) describe the morphology of cleaner fishes in Labridae and 2) document the kinematics of feeding in these taxa.

MATERIALS AND METHODS

Species

We gathered all data from juvenile individuals of three cleaner fishes in the Labridae: *L. dimidiatus* (Valenciennes, 1839) (standard length [SL] = 40.25–60.12 mm), *L. quadrilineatus* (Rüppell, 1835) (SL = 36.12-52.42 mm), and *T. lutescens* (Lay and Bennet, 1839) (SL = 50.20–83.98 mm). We examined juvenile individuals (identified by size and coloration pattern) because two of the species of interest clean facultatively as juveniles, while *L. dimidiatus* is an obligate cleaner, cleaning throughout its life history. We obtained all individuals ($n = 5$ per species, 15 individuals total) through the aquarium trade. We housed and filmed animals at the Long Marine Laboratory, University of California, Santa Cruz (IACUC #1009).

Collection of Kinematic Data

We used a Photron FASTCAM SA3 high-speed video camera (Photron, Tokyo) fitted with a macro lens to record each individual's feeding behaviors at 1,000 frames/sec in 1,024 × 1,024 resolution. All individuals were subject to each of two feeding treatments: 1) suspended client fishes and 2) attached invertebrates. We recorded feeding behaviors only after individuals were fully accustomed to feeding in each treatment type (typically 2–4 days). After each feeding trial, we recorded a still image of a ruler placed in the water column, for scale, without adjusting the camera's position, focus, or zoom level.

For the suspended client fishes treatment, we first euthanized individuals of *Chromis viridis* and *Dascyllus reticulatus* purchased from the aquarium trade, and wild-caught *Oxyjulis californica*. We then immediately froze them to preserve the mucus coating and/or ectoparasite loads on these potential client fishes. During feeding trials, we randomly selected a potential client and suspended it in the water column using a wire (Supporting Information S-Fig. 1A). Over the course of our study, we presented each individual cleaner fish with at least three individuals of each species of client fish. We presented each suspended client to the cleaner for no more than 7 min in order to mimic a typical maximum duration of such interactions in the wild (Hobson, 1971; Grutter, 1995; Grutter, 1996; Cole, 2010).

For the attached invertebrates treatment, we fed all individuals a mix of bloodworms and mysis shrimp attached to a substrate. We combined thawed mixtures of these prey items and then manually embedded the prey onto a wire mesh. We then suspended this wire mesh into the water column for feeding (Supporting Information S-Fig. 1B).

We digitized a total of 138 feeding sequences using the program Tracker 4.87 (Brown, 2009). For the attached

invertebrates treatment, we analyzed a total of 90 sequences (six sequences per individual fish). For the suspended client fishes treatment, we analyzed a total of 48 sequences (six sequences per individual fish), because not every individual cleaner fish engaged in cleaning during these trials. We only analyzed sequences in which 1) a successful strike occurred, 2) we were able to capture a completely lateral view of the feeding event, and 3) the fish's cranial axis was perpendicular to the camera. We considered trials successful when a fish removed an ectoparasite, scale, or some detritus from the suspended client, or a piece of bloodworm or shrimp from the wire mesh. We defined time zero (t_0) as the onset of the strike: the frame previous to that which showed initial jaw opening. We defined the end of the strike as the frame in which the jaws returned to their initial, prefeeding positions.

To quantify kinematic variables, we used seven landmarks on the external anatomy of the fish, following a slight modification of the procedure used by Ferry-Graham et al. (2002) on other labrids. These homologous landmarks (Fig. 1) were: 1) the anterior tip of the premaxilla, 2) the posterior margin of the nasal bone, 3) the (approximate) point of articulation between the hyomandibula and the neurocranium, 4) the dorsal margin of the insertion of the pelvic fin, 5) the anteroventral protrusion of the hyoid, 6) the (approximate) articulation of the lower jaw with the quadrate (i.e., the jaw joint), and 7) the anterior tip of the dentary (lower jaw). Using automated object tracking in Tracker (which we manually checked for error), we then used changes in the positions of these landmarks to gather data for three displacement variables, three angular variables, and eight timing variables. We digitized landmarks in every frame, and thus, we calculated all variables at every 1-ms interval.

The displacement variables we calculated were gape distance, premaxillary protrusion, and hyoid depression (all to the nearest 0.01 mm). We defined gape distance as the estimated distance between upper and lower jaw tips (Points 1 and 7 in Fig. 1). We calculated premaxillary protrusion as the net change in straight-line distance between the upper jaw tip and the posterior margin of the nasal bone (Points 1 and 2 in Fig. 1). We calculated hyoid displacement as the net change in straight-line distance between the anteroventral protrusion of the hyoid and the approximate point of articulation of the hyomandibula with the neurocranium (Points 3 and 5 in Fig. 1).

We calculated the three angular variables (in degrees): lower jaw rotation, cranial elevation, and girdle rotation. We defined each of these variables as the net change in an angle relative to its starting position at time t_0. Because there was minimal rotation in Point 3, we used it as a reference point. The angle we used to calculate lower jaw rotation was measured using Points 3, 6 (vertex), and 7 (Fig. 1). For cranial elevation, we calculated the angular rotation of Point 2 with respect to Point 3. We defined girdle rotation as the angular rotation of Point 4 with respect to Point 3 (Supporting Information S-Fig. 2). In calculating both cranial elevation and girdle rotation, we used an additional point to define the angular rotations. This additional point did not correspond to a discrete landmark. Rather, it varied across videos, but was chosen to be a point on the fish's body that 1) did not rotate, and 2) we could reliably find in each frame of the video. While we were interested in capturing the degree of pectoral girdle retraction, we found that the flapping of the pectoral fins often obscured the positions of features on the pectoral girdle. Only in a subset of our videos ($n = 17$; seven for *L. dimidatus*, five for *Larabicus*, five for *T. lutescens*) did the pectoral girdle's position remain clear throughout the feeding strike. We found that in these videos, the rotation of the pectoral girdle was remarkably correlated with the rotation of the pelvic fin insertion point within each species, as well as overall ($R^2 = 0.96$, slope = 1.003). We, therefore, chose to use the dorsal margin of the insertion of the pelvic fin (Point 4) as a proxy for the position of the pectoral girdle.

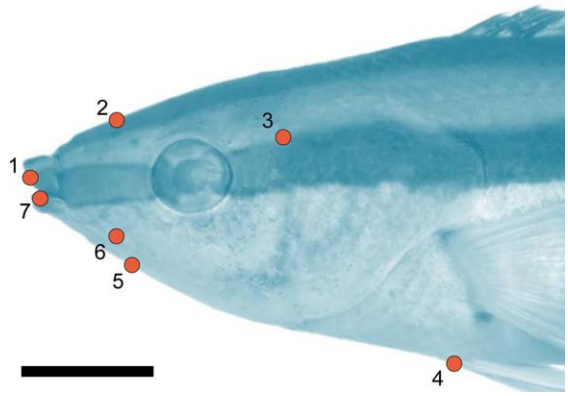

Fig. 1. Landmarks used during kinematic analyses. This lateral photograph of *L. dimidiatus* is faded for ease of viewing the following landmarks: 1) the anterior tip of the premaxilla, 2) the posterior margin of the nasal bone, 3) the (approximate) point of articulation between of the hyomandibula and the neurocranium, 4) the dorsal margin of the insertion of the pelvic fin (a reference point), 5) the anteroventral protrusion of the hyoid, 6) the (approximate) articulation of the lower jaw with the quadrate (i.e., the jaw joint), and 7) the anterior tip of the dentary (lower jaw). Scale bar = 5 mm.

The timing variables (ms) were: 1) time to peak gape, 2) time to peak premaxillary protrusion, 3) time to peak lower jaw rotation, 4) time to peak cranial elevation, 5) time to peak hyoid displacement, 6) time to prey contact (adduction of the jaws), 7) time to peak girdle rotation, and 8) time to full jaw retraction (i.e., the end of the strike).

In addition, we measured the body orientation angle at the onset of the strike by measuring the angle between the midline of the fish's cranium and the surface of the suspended wire mesh or client fish, with the vertex defined at the point where the strike occurred (Supporting Information S-Fig. 3).

Comparisons of Feeding Kinematics

In order to further explore the diversity of kinematic patterns shown by cleaners, we used a principal components analysis (PCA). For the PCA, we used 13 kinematic variables: (timing): time to peak gape, time to peak premaxillary protrusion, time to peak lower jaw rotation, time to peak cranial elevation, time to peak hyoid displacement, and time to complete jaw retraction; (displacement): peak gape distance, peak premaxillary protrusion distance, peak lower jaw rotation, peak cranial elevation, peak girdle rotation, peak hyoid displacement, and body orientation angle. We used each individual fish's mean data for all of these variables from each treatment. Because the data set comprised timing variables, linear measurements, and angles, we factored the correlation matrix of the variables in the PCA.

Following Jolicoeur (1963), when a PCA is computed using a nonsize-corrected data set, the first principal component (PC1) represents the line of best fit to the multivariate data (Pearson, 1901), and size is considered a latent variable that affects all variables simultaneously. We thus considered PC1 to capture the effects of body size on kinematics, while subsequent PCs capture other aspects of kinematic variation. We report only the PCs that cumulatively accounted for up to 95% of the total variation. We did not seek to incorporate phylogenetic information into the PCA, given that we were interested in exploring intraspecific variation.

To test for differences in mean kinematic profiles between species-treatment combinations, we conducted a multivariate analysis of variance (MANOVA) using scores from PCs 2–4 as the dependent variables. Using these scores allowed us to

conduct our comparative analyses in a manner that minimized the effects of predator body size. We defined groups as data belonging to distinct feeding treatments within species, wherever possible. We then conducted a series of pairwise comparisons of group means, and evaluated significance based on Hotelling's T-Square values and *P*-values.

Collection of Morphological Data

After videography, we euthanized all specimens via an overdose of MS-222 (IACUC protocol 1006) and fixed them in 10% buffered formalin for 10–14 days before transferring them to 70% ethanol for short-term storage.

We followed Winterbottom (1974) for muscle identification and descriptions. We removed two muscles from each preserved fish: the mm. adductor mandibulae (AM), and the mm. sternohyoideus (SH). The AM complex is a set of muscles that is responsible for generating the force involved in powering the closing of the jaws during biting. The SH depresses the hyoid bar, causing buccal expansion, which in turn aids in the generation of suction forces (Lauder et al., 1986; Westneat, 1990). Contraction of the SH also places tension on the interopercular-mandibular ligament, which connects the anterior aspect of the interoperculum with the posteroventral portion of the articular, thus contributing to depressing the dentary. We weighed each muscle to the nearest 0.0001 g using a Secura 213-1S precision balance (Sartorius Stedim Biotech GmbH, Germany). We removed all sections of the AM from one side of the specimen except section A_{ω} (Winterbottom, 1974), and then weighed each section independently.

Following muscle dissections, we cleared and double-stained specimens for bone and cartilage following Dingerkus and Uhler (1977). We used cleared and double-stained specimens to make osteological descriptions, and our terminology follows Gregory (1933) and Tedman (1980a,b).

In wrasses, a four-bar linkage system in the anterior jaws guides the rotation of the maxilla and the protrusion of the premaxilla as the mandible is depressed (Westneat, 1990; Westneat, 1994). The maxillary kinematic transmission coefficient (KT) for this linkage system relates the amount of maxillary rotation produced by a given amount of lower jaw rotation. This ratio is analogous to the inverse of the mechanical advantage of simple lever systems. Following Westneat (1990), we calculated maxillary KT as the ratio between the degrees of maxillary rotation and the degrees of lower jaw rotation for each specimen, which results in a dimensionless number. Since the assessment of maxillary KT is sensitive to the starting position of the system (Hulsey and Wainwright, 2002), we measured all starting angles with the jaws closed. We then rotated the lower jaw into a fully depressed position to quantify the changes in the angles associated with the input and output to the four-bar system.

We measured three additional traits on cleared and stained specimens: vertical gape distance, premaxillary protrusion distance, and basihyal length. We used these morphological variables to normalize their corresponding kinematic variables (vertical gape distance, premaxillary protrusion distance, and hyoid displacement, respectively) when plotting kinematic profiles. Vertical gape distance was measured as the distance between each of the most anterior canine teeth on the upper and lower jaws when the mouth was fully open. Premaxillary protrusion distance was measured as the excursion distance of the anteriormost canine tooth on the premaxilla as the upper jaw travels rostrally when the lower jaw is depressed. For each of these measurements, we rotated the lower jaw into a fully depressed position without forcing it beyond natural extension. Basihyal length was measured as the anterior to posterior distance along the midline of the basihyal. Measurements were recorded to the nearest 0.01 mm using the program ImageJ 1.47 (Rasband, 2014).

RESULTS

Morphology of Labrid Cleaners

External features. All three species feature an elongate, fusiform body shape. While describing the external features of these species in detail is not a focus of this study, we do note, however, that both *L. dimidiatus* and its close relative *Larabicus* feature fleshy, tube-shaped lips (Fig. 2). Additionally, the lower lip of each of these species features a short cleft along the midline. This split in the lip effectively creates two distinct lobes, each of which is immediately anterior to a large canine tooth. Unlike these species, *T. lutescens* lacks fleshy lips and has no midline split.

Jaws. The three cleaner fishes show a diversity of jaw shape, particularly in the paired premaxillae. A notable feature of both *L. dimidiatus* and *Larabicus* is the ventrally oriented curvature of the alveolar process of the premaxilla (Fig. 3A,C). All teeth are located on the paired premaxillae and dentary. The anterior tips of each premaxilla and each dentary feature a single, large caniform tooth that is slightly recurved. Between each of these anterior caniform teeth and extending caudally lie several rows of smaller villiform teeth. These teeth only occupy an anterior portion of each premaxilla and dentary, over a region that extends no more than approximately one-third the length of each bone. Both species also have a single caniform tooth located on the ateromedial face of the distal end of each alveolar process. These tusk-like teeth are of similar size to those found on the anterior tips of the jaws. These teeth do not appear to have a cutting edge (Supporting Information S-Fig. 4).

Unlike the condition seen in *L. dimidiatus* and *Larabicus*, *T. lutescens* has premaxillae that feature relatively straight alveolar processes with no caniform teeth at the distal ends (Fig. 3E). Also, while both the premaxilla and the dentary are lined with caniform teeth; no villiform teeth are present. The largest teeth in *T. lutescens* occupy the most anterior portions of the upper and lower jaws, and feature a slightly recurved shape. Toward the posterior portions of these bones, the teeth become smaller, less recurved, and more rounded. Some of this roundedness could be blunting, possibly due to wear.

In all three species, the ascending process of the premaxilla slides over the premaxillary condyle of the maxilla as the jaws open and close. While the thickness of this ascending process tapers evenly in *L. dimidiatus* and *Larabicus*, there is a distinct protuberance toward the base of the ventral side of this process in *T. lutescens*. In all three species, the ascending process curves slightly ventrally at the distal end. A palatopremaxillary ligament (Tedman, 1980b; Fig. 4) joins the medial side of the palatine to the dorsal side of the ascending

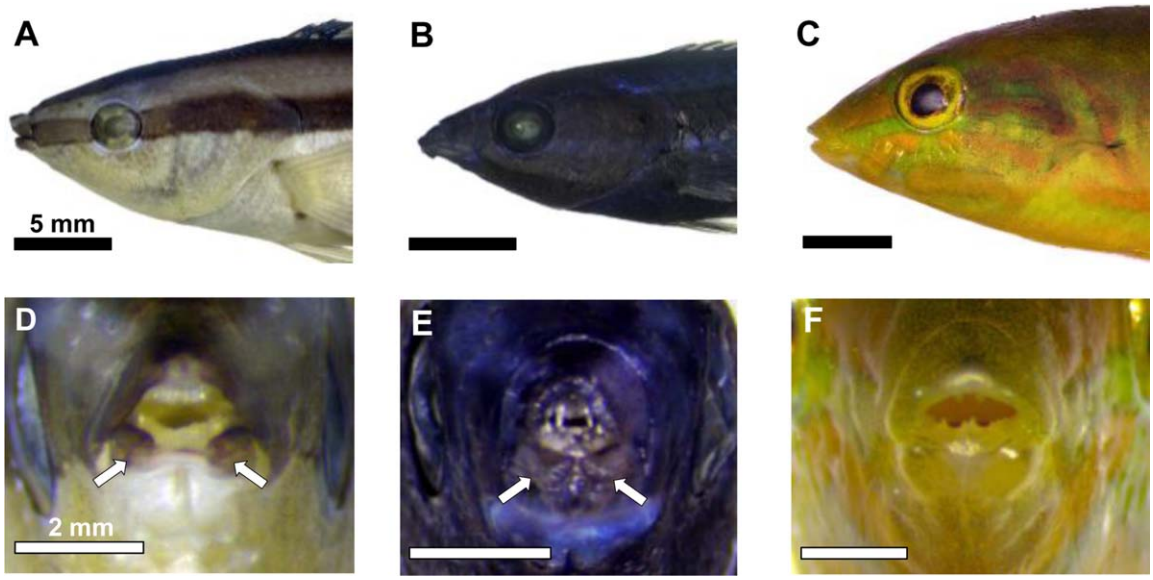

Fig. 2. Photographs of the external cranial morphology of three cleaner wrasses. Lateral photographs of *L. dimidiatus*, (**A**) *L. quadrilineatus*, (**B**) and *T. lutescens*; (**C**) black scale bars = 5 mm. (**D–F**) Anterior views of the lips and oral jaws of these species; white scale bars = 2 mm. *L. dimidiatus* (D) and *L. quadrilineatus* (E) each feature tube-shaped lips, with a vertical split in the lower lip along the midline. In D and E, white arrows point to distinct lobes on the lower lip, separated by the midline split. *T. lutescens* (F) lacks fleshy lips and has no midline split.

process of the premaxilla. A thick ligament, which we term the "quadrato-maxillary ligament," connects the anterior portion of the quadrate to the maxillary head (Fig. 4). As the jaws open, this ligament stabilizes the rotation of the maxilla, and appears to be the limiting factor in the extent of this rotation.

In all three species, the dentary articulates snugly with the horizontal process of the articular bone, and there is little to no flexion between the bones (Tedman, 1980a). As noted in other wrasses, an interoperculoarticular ligament connects the anterior edge of the interopercular to the posteroventral edge of the articular (Anker, 1986; Westneat, 1990).

In labrids, a set of ligaments connects the distal end of the maxillary arm, the alveolar process of the premaxilla, and the ascending process of the dentary, which Tedman (1980b) terms the "maxillodento-premaxillary complex." Anker (1986) specifies names for these ligaments, and Westneat (1990) describes them further. A premaxilla-maxillary ligament tethers the alveolar process of the premaxilla to the anterior edge of the distal end of the maxillary arm. A mandibular-maxillary ligament connects the distal end of the maxillary arm to the ascending process of the dentary. These ligaments, depicted in Figure 4, are present in all three cleaner fish species, attaching at similar points on their respective bones.

Maxillary KT. We found the maxillary KT of *L. dimidiatus* and *Larabicus* to be similar (0.70 and 0.62, respectively), while that of *T. lutescens* was slightly higher (0.99). We report species mean +/− SD for this trait in Table 1.

Hyoid. The hyoid apparatus consists of paired interhyals, epihyals, cerratohyals, hypohyals, and an unpaired basihyal and urohyal (Fig. 3). Unlike Tedman's (1980a) description of a single hypohyal bone in *L. dimidiatus*, we find two distinct bones: the hypohyal and the basihyal (Fig. 3B). The hypohyals are paired bones, short and rounded in appearance. The basihyal is the anteriormost bone in the hyoid apparatus, and takes the form of an elongate bar. This bone is relatively shorter in *L. dimidiatus* than in the other two taxa. In *T. lutescens*, the anterior tip of the basihyal is more broad and flat than that of the other two species.

The hyoid apparatus also supports the branchiostegal rays. *Larabicus* and *L. dimidiatus* each have five pairs of branchiostegal rays; *T. lutescens* has six. The first two pairs of branchiostegal rays are found on each medial face of the ceratohyals. All subsequent rays articulate with the lateral surfaces of the ceratohyals and epihyals.

Myology. We highlight the characteristics of the mm. AM and mm. SH muscles: The AM complex in labrids is composed of four muscles: A1, A2, A3, and Aω, which is also called the intramandibularis (Winterbottom, 1974; Tedman, 1980b). The intramandibularis originates on the medial face of the coronoid process of the articular and inserts on the ascending process of the dentary as well as the horizontal process of the articular

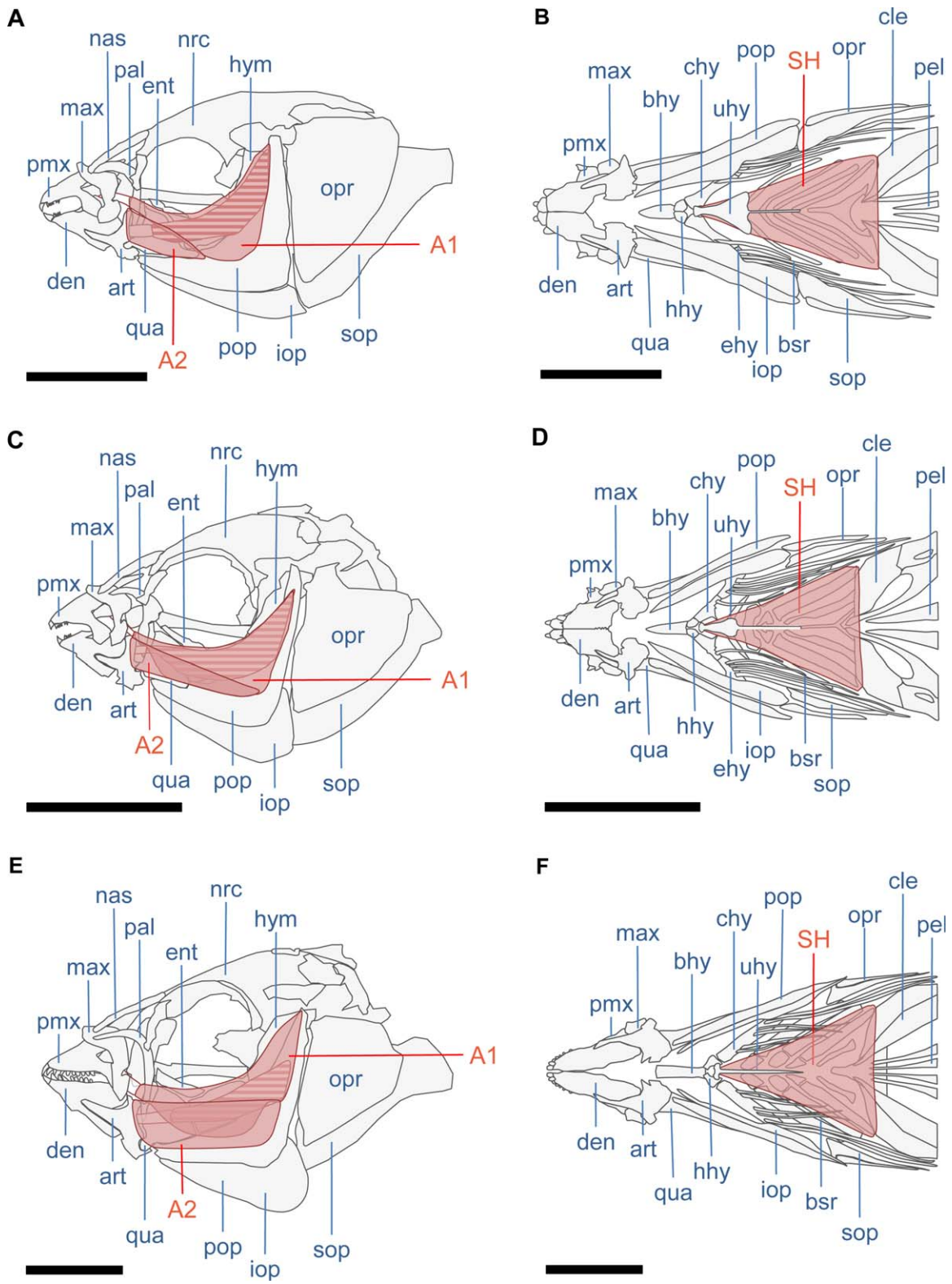

Fig. 3. Lateral and ventral views of cranial morphology of three cleaner wrasses. (**A**, **B**) *L. dimidiatus*; (**C**, **D**) *L. quadrilineatus*; (**E**, **F**) *T. lutescens*. Scale bars = 5 mm. AM muscles (A1, A2, A3) and SH muscles are also shown. AM muscles A1 and A2 overlie the more medial A3 (striped, unlabeled). Bone name abbreviations: art, articular; bhy, basihyal; bsr, branchiostegal rays; chy, ceratohyal; cle, cleithrum; den, dentary; ent, entopterygoid; hhy, hypohyal; hym, hyomandibula; iop, interopercle; max, maxilla; nas, nasal; nrc, neurocranium; opr, opercle; pal, palatine; pel, pelvis; pmx, premaxilla; qua, quadrate; sop, subopercle; uhy, urohyal.

(Tedman, 1980b). Due to its small size, especially in small juvenile fishes, we did not dissect out this muscle. All other muscle masses are reported in Table 1.

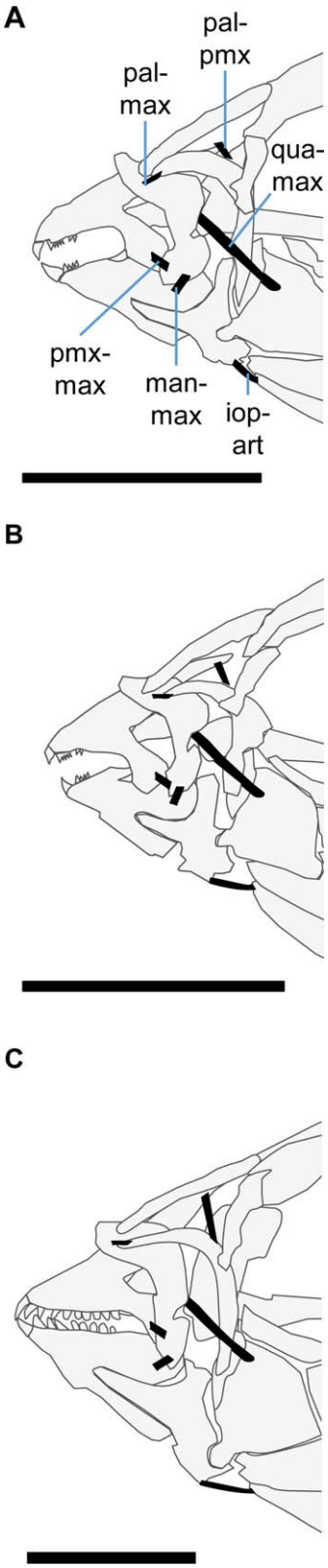

Following Winterbottom (1974), the defining characteristic of the A1 is that it inserts on the maxilla. In labrids, the A1 originates on the preopercle and quadrate bones and inserts on the premaxillary condyle of the maxilla via a long tendon and aponeurosis (Tedman, 1980b). It is of similar shape and relative size in all of the present taxa (Fig. 3, Table 1).

The A2 subdivision is the most superficial of the AM subdivisions (Fig. 3). Its origin is on the ventrolateral face of the quadrate and the anterolateral edge of the preopercle, in a more ventral location than that of the A1. It inserts onto the medial face of the coronoid process of the articular bone. In *L. dimidiatus*, the A2 is notably smaller (Table 1), and its origin is restricted to the quadrate.

The A3 is the most medial subdivision of the AM complex, covered predominantly by (A1 and partially by A2; Fig. 3). The A3 has two parts, as noted by Tedman (1980b). One part has a wide origin on the anterolateral edge of the preopercle, the hyomandibula, the metapterygoid, and the symplectic. The other part more narrowly originates on the hyomandibula and metapgerygoid. Both parts join together via an aponeurosis, which leads to a well-developed tendon (Tedman, 1980b). This large tendon inserts onto the medial surface of the articular. The A3 is similarly shaped in all three species (Fig. 3), although in *T. lutescens* it is disproportionately smaller by mass (Table 1).

The SH broadly originates on the cleithrum, with both the right and left sides tapering toward their anterior insertions on the urohyal (Winterbottom, 1974). This tapering gives the SH a roughly triangular shape in all three species (Fig. 3). We find, however, differences in muscle size; it appears to be substantially smaller in *L. dimidiatus*, while large in the sister species *Larabicus* when corrected for body size (Table 1).

Feeding Kinematics of Cleaners

During feeding trials in which we presented euthanized suspended client fishes to cleaners, not every cleaner fish interacted with the client. The largest two individuals of *Larabicus* (49.33 and 52.42 mm standard length) and all five individuals of *T. lutescens* consistently showed no interest in cleaning the variety of clients we presented throughout the study.

We thus report data from feeding behaviors of five *L. dimidiatus* and three *Larabicus* individuals.

Fig. 4. Lateral views of key ligaments in the feeding apparatus of three cleaner wrasses. (**A**) *L. dimidiatus*; (**B**) *L. quadrilineatus*; (**C**) *T. lutescens*. Scale bars = 5 mm. Ligament name abbreviations: iop-art, interopercular-articular; man-max, mandibular-maxillary; pal-max, palatomaxillary; pal-pmx, palatopremaxillary; pmx-max, premaxilla-maxillary; qua-max, quadrato-maxillary.

TABLE 1. Mean values for morphological data in three cleaner fishes

Species (# of individuals)	Standard length (mm)	A1 mass (g)	A2 mass (g)	A3 mass (g)	Total AM mass (g)	SH mass (g)	Maxillary KT	Vertical gape distance (mm)	Premaxillary protrusion distance (mm)	Basihyal length (mm)
Labroides dimidiatus ($n = 5$)	50.73 (8.20)	0.0045 (0.0012)	0.0024 (0.0005)	0.0047 (0.0011)	0.0116 (0.0026)	0.0065 (0.0036)	0.70 (0.06)	2.94 (0.20)	1.12 (0.15)	1.04 (0.17)
Larabicus quadrilineatus ($n = 5$)	42.86 (7.47)	0.0032 (0.0020)	0.0017 (0.0011)	0.0033 (0.0022)	0.0082 (0.0052)	0.0177 (0.0053)	0.62 (0.04)	2.49 (0.19)	0.71 (0.11)	1.00 (0.21)
Thalassoma lutescens ($n = 5$)	68.18 (12.88)	0.0184 (0.0103)	0.0091 (0.0047)	0.0077 (0.0038)	0.0352 (0.0187)	0.0391 (0.0225)	0.99 (0.05)	3.70 (0.27)	2.95 (0.33)	2.32 (0.24)

Mean values and standard deviations (in parentheses) are reported. Values for Maxillary KT, Vertical Gape Distance, Premaxillary Protrusion Distance, and Basihyal Length were measured on cleared and stained specimens. Maxillary KT is a dimensionless ratio (see Methods). AM: Adductor Mandibulae; KT: Kinematic Transmission Coefficient; SH: Sternohyoideus.

These individuals showed immediate interest in the client fish upon presentation, making repeated feeding strikes upon the client's body within the first few minutes. Individuals from both species consistently showed the ability to feed on suspended clients from a variety of positions, including those in which the predator was completely inverted (Supporting Information S-Fig. 2D). Generally, each cleaner fish lost interest in the suspended client after 3–5 min of interaction. We present prey capture kinematics for these cleaner fishes in Tables 2 and 3.

In contrast to the behaviors, we observed during the suspended client fishes treatment, all individuals readily fed on attached invertebrates. Here, every individual captured prey via biting; in each video, the oral jaws made direct contact with the prey item. Fishes from all three species showed rapid and multiple gape cycles in which individual invertebrates were targeted (Tables 2 and 3; Fig. 5).

Comparisons of Prey Capture Kinematics. We used data from six feeding strikes per feeding treatment, per individual. Through PCA, we found that four axes of variation cumulatively accounted for 95% of the total variance in the dataset (Table 4). All 13 variables loaded strongly onto PC1, and the eigenvectors were all in the same direction. This result fits Joliceur's characterization of the "size axis," wherein size is a latent factor that affects all variables (Jolicoeur, 1963).

We found that PCs 2 through 4 capture the majority of kinematic variation unrelated to size. Notably, all timing variables loaded negatively on all three of these axes. On PC2, which accounted for 16.52% of total variation, peak hyoid displacement, body orientation angle, and peak girdle rotation loaded strongly and positively. A variety of other traits loaded negatively on this axis, albeit weakly, including peak lower jaw rotation, and peak premaxillary protrusion distance. It is along this axis that species were generally separated (Fig. 6). On PC3 (3.83%), peak gape distance and body orientation angle loaded the most strongly. This axis revealed some sources of intraspecific variation, as indicated by the spread of individuals (especially in *T. lutescens*) in Figure 6.

Our MANOVA confirmed that groups within PCs 2–4 generally showed statistically significant differences in mean values (Wilk's $\lambda = 0.007$, $F_{12,42} = 20.015$, P-value < 0.001). An all-pairs comparison, however, revealed that not all pairs of groups showed significant differences (Table 5). Comparisons between feeding treatments within both *L. dimidiatus* and *Larabicus* did not show significant differences. All other pairs of species-treatment groups showed significant differences in means (all P-values < 0.003).

Kinematics of Prey Capture on Suspended Client Fishes. In *L. dimidiatus*, we found prey

TABLE 2. Mean values for timing variables in kinematic analyses in three cleaner fishes

Treatment *Species* (# of individuals)	Time to peak gape (ms)	Time to peak premaxillary protrusion (ms)	Time to peak lower jaw rotation (ms)	Time to peak hyoid displacement (ms)	Time to peak cranial elevation (ms)	Time to prey bite (ms)	Time to peak girdle rotation (ms)	Time to jaw retraction (ms)
Suspended clients								
Labroides dimidiatus ($n = 5$)	10.40 (0.20)	11.23 (0.33)	10.40 (0.20)	14.16 (0.52)	14.67 (0.63)	19.47 (0.76)	19.86 (1.34)	30.23 (2.00)
Larabicus quadrilineatus ($n = 3$)	11.17 (0.21)	11.00 (0.57)	11.17 (0.27)	16.28 (0.29)	16.28 (0.19)	24.01 (0.52)	21.37 (1.07)	31.50 (1.89)
Attached invertebrates								
Labroides dimidiatus ($n = 5$)	10.27 (0.24)	11.28 (0.11)	10.27 (0.24)	14.37 (0.71)	15.00 (0.67)	20.02 (0.53)	20.08 (1.23)	30.27 (1.89)
Larabicus quadrilineatus ($n = 5$)	11.17 (0.19)	11.00 (0.62)	11.17 (0.19)	16.20 (0.22)	16.20 (0.22)	23.78 (0.19)	21.76 (0.99)	32.28 (1.15)
Thalassoma lutescens ($n = 5$)	14.78 (0.18)	21.76 (0.38)	20.32 (0.17)	25.48 (0.37)	25.54 (0.82)	24.48 (0.29)	36.34 (2.45)	57.90 (2.60)

Mean values and standard errors (in parentheses) are reported for each kinematic variable related to timing within each treatment.

TABLE 3. Mean values for excursion distances and rotations in kinematic analyses in three cleaner fishes

Treatment *Species* (# of individuals)	Peak gape distance (mm)	Peak premaxillary protrusion distance (mm)	Peak hyoid displacement (mm)	Peak lower jaw rotation (°)	Peak cranial elevation (°)	Peak girdle rotation (°)	Body orientation angle (°)
Suspended clients							
Labroides dimidiatus ($n = 5$)	1.27 (0.05)	0.67 (0.06)	0.15 (0.01)	13.33 (0.28)	2.86 (0.35)	2.16 (0.33)	45.25 (0.28)
Larabicus quadrilineatus ($n = 3$)	1.42 (0.12)	0.32 (0.09)	0.26 (0.03)	11.54 (0.33)	4.17 (0.27)	2.87 (0.31)	63.02 (0.52)
Attached invertebrates							
Labroides dimidiatus ($n = 5$)	1.26 (0.08)	0.67 (0.06)	0.16 (0.01)	13.02 (0.42)	2.52 (0.23)	2.17 (0.26)	58.29 (0.63)
Larabicus quadrilineatus ($n = 5$)	1.41 (0.18)	0.33 (0.08)	0.26 (0.02)	11.69 (0.19)	3.24 (0.34)	3.42 (0.27)	64.14 (0.75)
Thalassoma lutescens ($n = 5$)	3.11 (0.54)	2.36 (0.36)	0.25 (0.01)	25.88 (0.43)	5.34 (0.20)	2.78 (0.26)	70.02 (1.24)

Mean values and standard errors (in parentheses) are reported for each kinematic variable related to excursion distance or rotation within each treatment.

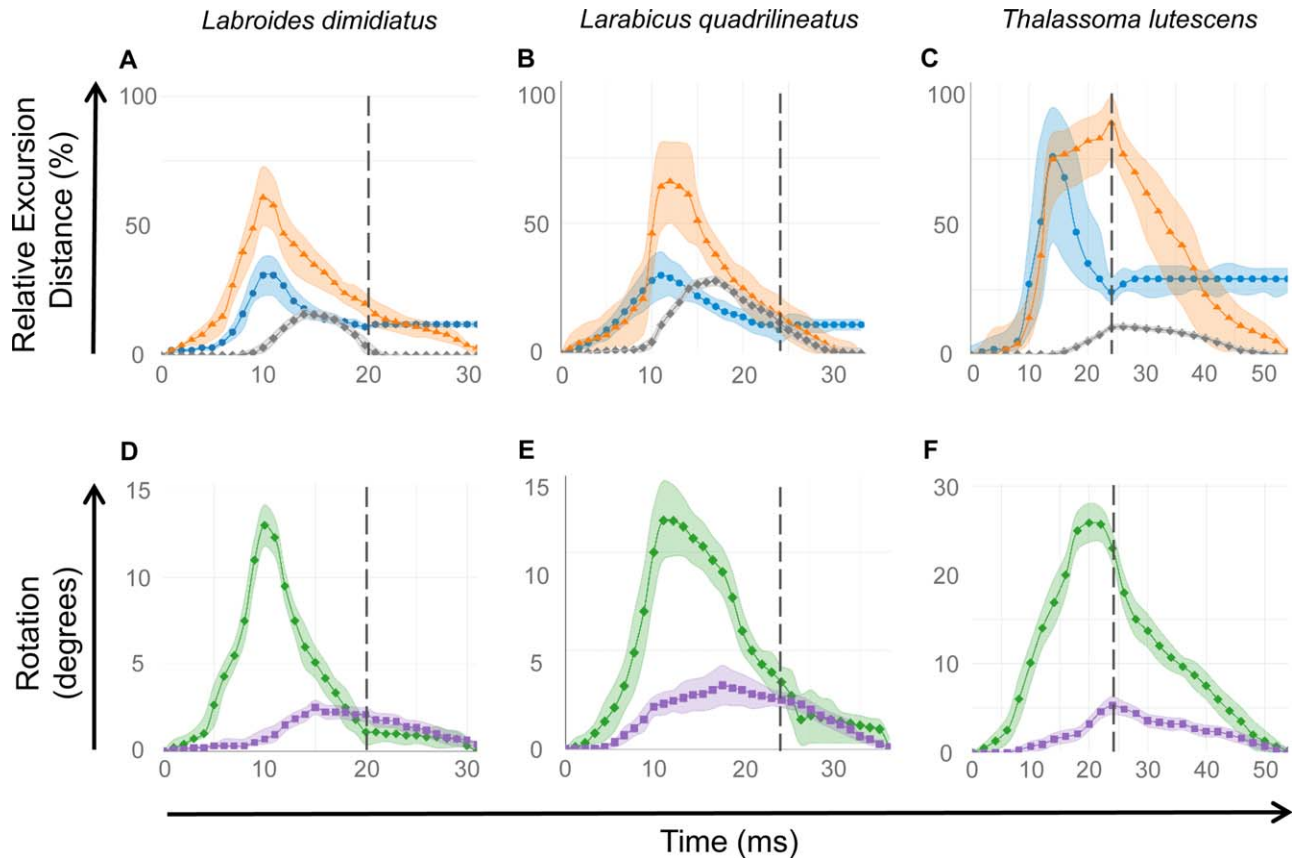

Fig. 5. Kinematic profiles of three cleaner fishes feeding on attached invertebrates. Profiles illustrate kinematics of (**A**, **D**) *L. dimidiatus*, (**B**, **E**) *L. quadrilineatus*, and (**C**, **F**) *T. lutescens*. All profiles depict mean +/− s.e. values after adjusting for size. Data are from the embedded invertebrates treatment, across all individuals within a species. Dashed vertical lines show the mean time at which prey capture occurred via biting. In A–C, blue circles indicate data for gape excursion, orange triangles indicate data for premaxillary protrusion distance, and gray diamonds indicate data for hyoid displacement. These kinematic variables are normalized by their corresponding morphological variables, (measured on cleared and stained specimens): vertical gape distance, premaxillary protrusion distance, and basihyal length, respectively. We calculated gape excursion as the gape distance at time *t* minus the initial gape distance. This accounts for the space between the jaws before the onset of the strike, and represents the actual distance the jaws travel. Standard error in hyoid displacements is relatively small (see Table 3); thus, errors (shading) are not fully visible. In D–F, green diamonds indicate data for lower jaw rotation, and purple squares for cranial rotation.

capture events were rapid, with gape cycles (i.e., the time between jaw opening and full jaw retraction) lasting 30.2 +/− 2.00 ms s.e. (Table 2). Individuals of this species showed modest excursion distances (Table 3) for peak gape (1.27 +/− 0.05 mm s.e.), peak premaxillary protrusion (0.67 +/− 0.06 mm s.e.), and also extremely small excursions for peak hyoid displacement (0.15 +/− 0.01 mm s.e.). These low-displacement events were coupled with modest rotations; peak jaw rotation was 13.33 +/− 0.28° s.e., peak cranial rotation was 2.86 +/− 0.35° s.e., and peak girdle rotation was 2.16 +/− 0.33° s.e. The timing of peak jaw rotation was synchronous with peak gape excursion in every video we analyzed (Supporting Information S-Video 1). During prey capture events, *L. dimidiatus* individuals maintained an acute body orientation angle (45.25 +/− 0.28° s.e.).

In *Larabicus*, we also found prey capture events to be rapid, with gape cycles lasting 31.5 +/− 1.89 ms s.e. (Table 2). Individuals of this species showed modest excursion distances (Table 3) for peak gape (1.42 +/− 0.12 mm s.e.), peak premaxillary protrusion (0.32 +/− 0.09 mm s.e.). Peak hyoid displacement, however, was higher (0.26 +/− 0.03 mm s.e.) than that shown in *L. dimidiatus*. Again, the low-displacement events were coupled with modest rotations; peak jaw rotation was 11.54 +/− 0.33° s.e., peak cranial rotation was 4.17 +/− 0.27° s.e., and peak girdle rotation was 2.87 +/− 0.31° s.e. As in *L. dimidiatus*, the timing of peak jaw rotation was synchronous with peak gape excursion in every video we analyzed (Supporting Information S-Video 2). During prey capture events, *Larabicus* individuals maintained an acute body orientation angle (63.02 +/− 0.52° s.e.).

Kinematics of Feeding on Attached Invertebrates. In this treatment, we identified a clearer role of suction in prey capture in *L. dimidiatus* and *Larabicus*. As the jaws opened, we

TABLE 4. PCA on kinematic variables reveals axes of variation in the feeding behaviors of three cleaner fishes

Principal component (% variance)	PC 1 (72.20%)	PC 2 (16.52%)	PC 3 (3.83%)	PC 4 (3.08%)
Time to peak gape	**0.975**	−0.027	−0.013	−0.046
Time to peak premaxillary protrusion	**0.960**	−0.242	−0.076	−0.035
Time to peak lower jaw rotation	**0.984**	−0.125	−0.033	−0.063
Time to peak cranial elevation	**0.971**	−0.076	−0.161	−0.053
Time to peak hyoid displacement	**0.973**	−0.028	−0.161	−0.092
Time to complete jaw retraction	**0.960**	−0.122	−0.034	−0.139
Peak gape distance	**0.868**	0.048	**0.425**	0.368
Peak premaxillary protrusion distance	**0.893**	−0.282	0.261	0.270
Peak hyoid displacement	**0.471**	**0.777**	0.023	−0.023
Peak lower jaw rotation	**0.924**	−0.314	−0.025	0.025
Peak cranial elevation	**0.785**	0.171	0.222	−0.137
Peak girdle rotation	**0.423**	**0.863**	0.299	−0.181
Body orientation angle	**0.457**	**0.750**	**−0.441**	0.263

We used each individual fish's mean data from each treatment in the PCA. Only the first four principal components are described here. Table entries are the loadings for variables (i.e., correlations between each variable and each principal component). Loadings in bold are strong (i.e., $|\text{loading}| > 0.4$).

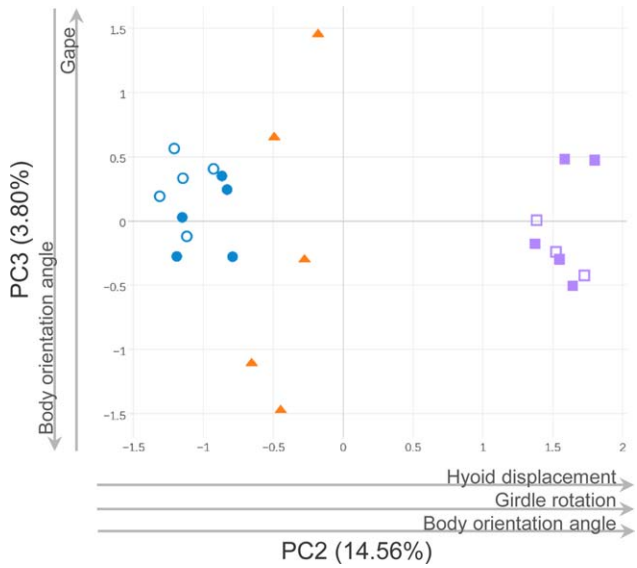

Fig. 6. Axes of kinematic variation in prey capture as revealed by PCA for three cleaner fish species. Symbols on the scatterplot represent five individuals per species. Blue circles represent *L. dimidiatus* individuals, orange diamonds represent *T. lutescens* individuals, and purple squares represent *L. quadrilineatus* individuals. Open symbols correspond to data from the suspended clients treatment, while filled symbols depict data from the attached invertebrates treatment. Variables that loaded strongly on each axis are represented by arrows that indicate the direction in which the variables increase along the axis. See Table 4 for additional information on loadings and text for discussion.

inferred suction generation by each of these species by noting that the invertebrate prey were immediately pulled toward the mouth of the predator. This suction force was rarely sufficient to overcome the prey's attachment to the wire mesh apparatus. In order to maintain consistency, we gathered kinematic data only from videos in which biting was employed to capture prey.

TABLE 5. Hypothesis testing of all pairs of species-treatment means via MANOVA

Group_i	Group_j	Hotelling's T-square	*P*-value
Lab dim AI	Lab dim SC	4.462	0.212
Lab dim AI	Tha lut AI	32.922	**<0.003**
Lab dim AI	Lar qua AI	653.623	**<0.001**
Lab dim AI	Lar qua SC	481.155	**<0.001**
Lab dim SC	Tha lut AI	60.951	**<0.001**
Lab dim SC	Lar qua AI	761.039	**<0.001**
Lab dim SC	Lar qua SC	561.491	**<0.001**
Tha lut AI	Lar qua AI	393.894	**<0.001**
Tha lut AI	Lar qua SC	288.122	**<0.001**
Lar qua AI	Lar qua SC*	0.255	0.901

For the MANOVA, we used scores from principal components 2, 3, and 4 as the dependent variables. We defined groups as data belonging to distinct feeding treatments within species. Group names use the first three letters of the genus and species name (e.g. *Labroides dimidiatus* = Lab dim), followed by an abbreviation for the treatment (AI: Attached Invertebrates; SC: Suspended Clients). Each group thus contained data from five individuals of the species, except the group marked (*), which contained data from three individuals. We obtained Hotelling's T-Square values and *P*-values via an all-pairs comparison of group means. Significant differences ($\alpha = 0.05$; *P*-value ≤ 0.05) between group means are indicated by bold *P*-values.

In both of these taxa, we found the kinematic patterns to be similar to those in the suspended client fishes treatment (Supporting Information S-Video 3, 4). These species again achieved prey capture through low-displacement events (Table 3; Fig. 5A,B). Peak gape was 1.26 +/− 0.08 mm s.e. and peak jaw protrusion was 0.67 +/− 0.06 mm s.e. in *L. dimidiatus*. In *Larabicus*, peak gape was (1.41 +/− 0.18 mm s.e.) and peak jaw protrusion was 0.33 +/− 0.08 mm s.e.). These low-displacement events again were coupled with small rotations in the lower jaw and cranial skeleton (Fig. 5D,E). Peak jaw rotation was 13.02 +/− 0.42° s.e., peak cranial rotation was 2.16 +/− 0.33° s.e., and peak girdle rotation was 2.17 +/− 0.26° s.e. in *L. dimidiatus*. In *Larabicus*, peak jaw

rotation was 11.69 +/− 0.19° s.e., peak cranial rotation was 3.24 +/− 0.34° s.e., and peak girdle rotation was 3.42 +/− 0.27° s.e. These species also showed acute body orientation angles during prey capture; *L. dimidiatus*: 58.29 +/− 0.63° s.e., *Larabicus*: 64.14 +/− 0.75° s.e.

While also successfully targeting individual invertebrate prey, *T. lutescens* exhibited a kinematic pattern divergent from that of the other cleaners (Fig. 5C,F). Jaw movements were generally slower in *T. lutescens*, with time to peak gape occurring at 14.78 +/− 0.18 ms s.e., and time to peak premaxillary protrusion occurring at 21.76 +/− 0.38 ms s.e. (Table 2). Unlike in the other taxa, the timing of peak jaw rotation in *T. lutescens* was not synchronous with peak gape excursion, but rather showed synchrony with the time to peak premaxillary protrusion (Supporting Information S-Video 5). The excursion distances of peak gape (3.11 +/− 0.54 mm s.e.) and peak premaxillary protrusion (2.36 +/− 0.36 mm s.e.) were higher than those seen in the other cleaners, in part due to the larger body size of the *T. lutescens* individuals in this study (Table 3). This species also showed larger rotation values; peak jaw rotation was 25.88 +/− 0.43° s.e., peak cranial rotation was 5.34 +/− 0.20° s.e., and peak girdle rotation was 2.78 +/− 0.26° s.e. These larger values for kinematic traits correspond to the higher maxillary KT values we found for *T. lutescens* (Table 1). Finally, *T. lutescens* did not exhibit as acute body orientation angles (70.02 +/− 1.24° s.e.) as the other species.

DISCUSSION

The kinematic patterns we quantified inform our understanding of the functional morphology of cleaners. In each feeding event, only single prey items (e.g., a single bloodworm, ectoparasite, or fish scale) were targeted, although often many were present. We find that all individuals in our study predominately captured prey via biting; in nearly every video, the upper and lower jaws made direct contact with the prey item (Alfaro et al., 2001).

Larabicus and *L. dimidiatus* show similarity in kinematic profiles, perhaps in part due to their close relatedness. In these species, individuals used the smaller, anteromedial villiform teeth to bite into the prey, rather than the larger anterior canines. The relatively acute body orientation angles (see Table 3) these species exhibited during prey capture allow the anteromedial teeth of the lower jaw to contact the prey via the split in the lower lip. Interestingly, individuals of *L. dimidiatus* approached suspended clients at slightly more acute body orientation angles than they did the wire mesh with attached invertebrates.

The curve of the alveolar process of the premaxillae in *L dimidiatus* and *Larabicus* ensures that only the anteriormost teeth make contact with prey, confining the bite to a reduced area. We interpret the function of these jaw-closing kinematics to be analogous to using forceps, where one exerts precise and localized force to remove an object (Ferry-Graham et al., 2008). Once captured, the prey item occupies the space left open by the split in the lower lip. From our videos, the single caniform tooth at the distal end of each alveolar process of the paired premaxillae does not appear to contact prey. Whether this tooth plays a functional role in feeding in these species remains unclear.

In *T. lutescens*, individuals captured prey using only the anteriormost caniform teeth, which are relatively large and somewhat recurved. Although teeth occupy a larger proportion of the alveolar process length in this species, only the anteriormost teeth came into contact with prey. Perhaps because this species lacks small villiform teeth and tube-shaped lips, *T. lutescens* is less likely to exhibit an acute body orientation angle.

In all three species, the lower jaw acts as one functional unit, and no intramandibular joint (IMJ; Konow and Bellwood, 2005; Konow et al., 2008; Ferry-Graham and Konow, 2010; Konow and Bellwood, 2011) is present. The relationship between cleaning and bearing an IMJ is not straightforward. IMJs generally augment vertical gape expansion during biting. The only group within the Labridae with IMJs (scarids) contains no known cleaners. On the other hand, pomacanthid IMJs restrict the extent of the gape (Konow et al., 2008), and some pomacanthids clean, such as the emperor angelfish (*Pomacanthus imperator*; Kuiter, 1996; Konow et al., 2006). Given that cleaners exhibit small gapes (this study; Wainwright et al., 2004; Baliga and Mehta, 2014) it is possible that this gape-restricting mechanism plays an important role in the functional morphology of cleaning in pomacanthids.

In each species, suction generation also seems to play an important role in prey capture, often helping to orient the prey item toward the buccal cavity. In cases where the prey is weakly attached to a substrate, suction alone could be sufficient for capture. However, in cases where the prey remains strongly attached, the predator uses the anteriormost portion of its oral jaws to bite into and pull off the prey item. While we did not explicitly quantify suction forces, we suspect that *Larabicus* possesses greater suction capability than the other two species we examined. *Larabicus* has a relatively large SH, the bony elements of the hyoid in this species are well developed, and there is a substantial peak hyoid displacement during prey capture. Furthermore, *Larabicus* (regardless of feeding treatment) had the highest positive scores

on PC2 of our PCA. Peak hyoid displacement and peak girdle rotation both load strongly and positively on this axis, while all timing variables load negatively (albeit weakly). Since predators with enhanced suction capability are expected to show greater hyoid displacements and a higher velocity of cranial expansion (Gibb and Ferry-Graham, 2005), the loadings on PC2 lead us to characterize it as a "relative suction capability" axis. High positive scores for *Larabicus* on this axis reflect its underlying ability to generate enhanced suction.

Our three species of cleaner fishes show small jaw displacements during feeding. Our results correspond with our finding relatively low maxillary KT values for these species. The mean maxillary KT for *L. dimidiatus* in our study was 0.70. This measurement is close to that found in larger individuals of this species by Wainwright et al. (2004), a study focused on labrids around the Great Barrier Reef. When we compare across the 104 wrasses in the Wainwright et al. (2004) dataset, we find that *L. dimidiatus* is ranked in the lower quartile for maxillary KT. *Larabicus*, which is not present in the Wainwright et al. (2004) dataset, exhibits an even lower maxillary KT than *L. dimidiatus*. In addition, while we here find the maxillary KT of *T. lutescens* (0.99) to be higher than those of our other two cleaner species, this KT is far lower than those of similarly sized noncleaner congeners (Baliga and Mehta, 2014). In this study, we find that the low maxillary KT of our three species is associated with reduced displacement of the jaws (small gape, little premaxillary protrusion) during feeding.

These low-displacement events are coupled with fast timing values for all the variables we measured. Together, these findings indicate that the evolution of cleaning in labrids may be associated with selection toward the ability to perform low-displacement, fast jaw movements that allow for rapid gape cycles on individually targeted items. Given that cleaners consume prey that are embedded into a substrate (skin between scales), it may not only be advantageous, but also necessary to take multiple quick bites in order to dislodge prey. Bites that are too forceful (i.e., abrasive) could dissuade client fishes to wait around in time for the cleaner to consume prey. We find support for this hypothesis in our assessment of the morphology of the present cleaner wrasses. Juvenile *Larabicus* and *L. dimidiatus* possess small jaw-closing muscles, low kinematic transmission, and small premaxillary protrusion. Previous work has shown that juvenile *T. lutescens* (among other *Thalassoma* cleaners) also have small jaw-closing muscles and exhibit relatively weak bite forces when compared to juvenile noncleaner congeners (Baliga and Mehta, 2014).

The kinematic patterns in both *L. dimidiatus* and *Larabicus* were remarkably similar across feeding treatments, and the kinematics (timing, angular excursions, and displacements) were consistent across feeding strategies. Simply put, distinct feeding treatments within species did not lead to significant distinctions in feeding kinematics. While we were unable to solicit cleaning behavior from *T. lutescens*, we argue that the kinematic pattern that this species exhibits during our attached invertebrate feeding treatment could serve as a reasonable proxy; in both treatments, in this study, prey are attached to a substrate. Curiously, the two largest specimens of *Larabicus* (standard lengths 49.33 and 52.42 mm) also showed no interest in cleaning euthanized clients. While we have a low sample size in this study ($n = 5$), our findings confirm our assertion that the transition away from cleaning in this species likely occurs at a small size, probably around 45-mm standard length.

Picking

As documented by Ferry-Graham et al. (2008), cyprinodontiform taxa exhibit the ability to "pick" individual prey items from a substrate or water column. This is achieved through an unusual premaxillary protrusion mechanism, wherein the alveolar process of the premaxilla does not rotate anteriorly to occlude the sides of the open mouth during prey capture. Occluding the lateral sides of the mouth is considered to be important for generating suction (Ferry-Graham and Lauder, 2001; Day et al., 2005). Instead, a premaxillomandibular ligament restricts alveolar rotation, and the premaxilla slides anteroventrally along the length of its ascending process (Alexander, 1967; Hernandez et al., 2008).

In wrasses, a four-bar linkage system governs the movements of jaw opening and closing (Westneat, 1990; Westneat, 1994). While the premaxilla is not explicitly modeled as a component of this linkage system, its movements are guided by the rotation of the maxilla. Here, the alveolar process of the premaxilla typically rotates anteriorly during mouth opening due to the connection it shares with the alveolar process of the maxilla (the premaxilla-maxillary ligament; Fig. 4). The extent of this rotation varies as a function of each species' maxillary KT; in species with a larger maxillary KT value, the maxilla (and thus the premaxilla) exhibits greater rotation. However, similar to the condition seen in cyprinodontiforms, the alveolar process of the premaxilla is effectively pinned to the alveolar process of the maxilla. Because of this connection, the premaxilla acts as a sliding element that descends along the length of its ascending process during prey capture. While this mechanism of premaxillary protrusion is present in the three cleaner fish species in this study, it is also a feature of the majority of wrasses, and thus

is not exclusive to cleaners (Westneat, 1990; Westneat, 1994).

Another key aspect of picking observed in cyprinodontiforms is the apparent trade-off between the speed and the precision of the bite. Ferry-Graham et al. (2008) note that the precise picking behavior of taxa in their study requires slow, controlled jaw movements. The authors further argue that these features may be traded off for some aspects of suction-feeding performance, such as jaw-opening speed and protrusion distance. We converted the following approximate time to peak gape times from their study to ms: 20–30 ms in *Fundulus rubrifrons* and *Kryptolebias marmoratus* and 40–50 ms in *Poecilia sphenops* and *Gambusia affinis*. The kinematic profiles for these "picker" species also indicate the mean total strike time ranges from approximately 55 ms (in *Fundulus*) to approximately 145 ms (in *Gambusia*). These timing values are markedly slower than those seen in three species of percomorphs (*Betta splendens*, *Chaetodon xanthurus*, and *Syngnathus leptorhynchus*) highlighted in their study, results which the authors use to postulate that dexterity requires slow, precisely controlled jaw movements.

In this study, no such trade-off exists. Cleaners are fast, precise pickers that are capable of obtaining individual prey items. We find that while exhibiting excursions of a similar magnitude to those seen in cyprinodontiforms, cleaners achieve peak gape in 10–17 ms, and a full gape cycle between 32–55 ms. Effectively, all jaw movements of cleaner fishes are twice as fast as those seen in cyprinodontiform pickers. Suction generation also seems to play an important role in prey capture, and cleaner fishes appear to be capable of both speed and dexterity. Cleaners in our study were consistent in the timing of kinematic events, regardless of size or species identity (indicated by weak loadings of these variables on PCs 2–4). Cleaners are capable of fast jaw opening and fast jaw occlusion, which facilitates obtaining individual prey items embedded in a client.

CONCLUSION

The kinematic basis of cleaning behavior appears to be in rapid, low-displacement jaw movements. While notable suction forces are generated as the jaws open, the capture of securely attached prey relies on a biting behavior in which only the anterior tips of the jaws contact the prey. These mouth movements allow cleaners to selectively grasp individual prey items, akin to the "picking" seen in cyprinodontiform taxa. While the feeding styles of cleaners show notable similarity to those of cyprinodontiforms, we find key differences between these taxa in the timing of kinematic events. In fact, cleaners generally seem to be able to capture prey twice as fast as cyprinodontiforms. We thus suggest that the kinematic patterns exhibited by cleaners are indicative of picking behavior, but that "pickers" may be more kinematically diverse in timing than previously thought. Perhaps unsurprisingly, the closely related *L. dimidiatus* and *L. quadrilineatus* showed a high degree of similarity in traits. It is likely that studies on the morphology and feeding kinematics of cleaners in other labrid genera (e.g., *Symphodus*, *Halichoeres, Bodianus*, and *Coris*) will shed further light on the diversity of picking behaviors.

ACKNOWLEDGMENTS

The authors thank T. Portulano for help with digitizing landmarks on videos, and M. Mac for assistance with muscle dissections and some portions of the clearing & staining process. C.J. Law provided helpful discussion on the manuscript. The authors also thank two reviewers for their very insightful comments and helpful suggestions.

LITERATURE CITED

Alexander RMcN. 1967. The functions and mechanics of the protrusible upper jaws of some acanthopterygian fish. J Zool 151:43–64.

Alfaro ME, Janovetz J, Westneat MW. 2001. Motor control across trophic strategies: Muscle activity of biting and suction feeding fishes. Am Zool 41:1266–1279.

Anker GCh. 1986. The morphology of joints and ligaments in the head of a generalized Haplochrornis species: *H. elegans* Trewavas 1933 (Teleostei, Cichlidae). Neth J Zool 36:499–530.

Baliga VB, Mehta RS. 2014. Scaling patterns inform ontogenetic transitions away from cleaning in *Thalassoma* wrasses. J Exp Biol 217:3597–3606.

Brown D. 2009. Tracker Video Analysis and Modeling Tool (Version 4.87) [Computer software]. Retrieved Jan 2, 2015, Available at: http://www.cabrillo.edu/~dbrown/tracker/.

Cole AJ. 2010. Cleaning to corallivory: Ontogenetic shifts in feeding ecology of tubelip wrasse. Coral Reefs 29:125–129.

Coté IM. 2000. Evolution and ecology of cleaning symbioses in the sea. Oceanogr Mar Biol 38:311–355.

Cowman PF, Bellwood DR. 2011. Coral reefs as drivers of cladogenesis: Expanding coral reefs, cryptic extinction events, and the development of biodiversity hotspots. J Evol Biol 24: 2543–2562.

Darcy GH, Maisel E, Ogden TC. 1974. Cleaning preferences of the gobies *Gobiossoma evelynae* and *G. prochilos* and the juvenile wrasse *Thalassoma bifasciatum*. Copeia 1974:375–379.

Day SW, Higham TE, Cheer AY, Wainwright PC. 2005. Spatial and temporal flow patterns during suction feeding of bluegill sunfish (*Lepomis macrochirus*) by Particle Image Velocimetry. J Exp Biol 208:2661–2671.

Dingerkus G, Uhler DL. 1977. Enzyme clearing of Alcian blue-stained whole small vertebrates for demonstration of cartilage. Stain Technol 32:229–231.

Ferry-Graham LA, Konow N. 2010. The intramandibular joint in *Girella*: A mechanism for increased force production? J Morphol 271:271–279.

Ferry-Graham LA, Lauder GV. 2001. Aquatic prey capture in Ray-finned fishes: A century of progress and new directions. J Morphol 248:99–119.

Ferry-Graham LA, Wainwright PC, Westneat MW, Bellwood DR. 2002. Mechanisms of benthic prey capture in wrasses (Labridae). Mar Biol 41:819–830.

Ferry-Graham LA, Gibb AC, Hernandez LP. 2008. Premaxillary movements in cyprinodontiform fishes: An unusual protrusion

mechanism facilitates "picking" prey capture. Zoology 111: 455–466.
Froese R, Pauly D, editors. 2015. FishBase. World Wide Web electronic Publication, Kiel, Germany. Available at: www.fishbase.org, version (1/2015).
Gibb AC, Ferry-Graham L. 2005. Cranial movements during suction feeding in teleost fishes: Are they modified to enhance suction production? Zoology 108:141–153. (2015):
Gregory WK. 1933. Fish skulls: A study of the evolution of natural mechanisms. Trans Am Philos Soc 23:481 p.
Grutter AS. 1995. Relationship between cleaning rates and ectoparasite loads in coral reef fishes. Mar Ecol Prog Ser 118: 51–58.
Grutter AS. 1996. Parasite removal rates by the cleaner wrasse *Labroides dimidiatus*. Mar Ecol Prog Ser 130:61–70.
Hernandez LP, Ferry-Graham LA, Gibb AC. 2008. Morphology of a picky eater: A novel mechanism underlies premaxillary protrusion and retraction within cyprinodontiforms. Zoology 111:442–454.
Hernandez LP, Gibb AC, Ferry-Graham LA. 2009. Trophic apparatus in cyprinodontiform fishes: Functional specializations for picking and scraping behaviors. J. Morphol 270:645–661.
Hobson ES. 1971. Cleaning symbioses among California inshore fishes. Fish Bull 69:491–523.
Horn MH, Ferry-Graham LA. 2006. Feeding mechanisms and trophic interactions. In: Allen LG, Pondella DJ, Horn MH, editors. The Ecology of Marine Fishes: California and Adjacent Waters. Berkeley: University of California Press. pp 397–410.
Hulsey CD, Wainwright PC. 2002. Projecting mechanics into morphospace: Disparity in the feeding system of labrid fishes. Proc R Soc B 269:317–326.
Jolicoeur P. 1963. The multivariate generalization of the allometry equation. Biometrics 19:497–499.
Konow N, Bellwood DR. 2005. Prey-capture in *Pomacanthus semicirculatus* (Teleostei, Pomacanthidae): Functional implications of intramandibular joints in marine angelfishes. J Exp Biol 208:1421–1433.
Konow N, Bellwood DR. 2011. Evolution of high trophic diversity based on limited functional disparity in the feeding apparatus of marine angelfishes (f. Pomacanthidae). PloS One 6: e24113.
Konow N, Fitzpatrick R, Barnett A. 2006. Adult Emperor angelfish (*Pomacanthus imperator*) clean Giant sunfishes (*Mola mola*) at Nusa Lembongan, Indonesia. Coral Reefs 25: 208–208.
Konow N, Bellwood DR, Wainwright PC, Kerr AM. 2008. Evolution of novel jaw joints promote trophic diversity in coral reef fishes. Biol J Linn Soc 93:545–555.
Kuiter RH. 1996. Guide to the Sea Fishes of Australia. Sydney: New Holland.
Lauder GV, Wainwright PC, Findeis E. 1986. Physiological mechanisms of aquatic prey capture in sunfishes: Functional determinants of buccal pressure changes. Comp Biochem Physiol 84A:729–734.
Liem KF. 1979. Modulatory multiplicity in the feeding mechanism in cichlid fishes, as exemplified by the invertebrate pickers of Lake Tanganyika. J Zool Lond 189:93–125.
Losey GS, Balazs GH, Privitera LA. 1994. Cleaning symbiosis between the wrasse, *Thalassoma duperrey*, and the green turtle, *Chelonia mydas*. Copeia 684–690.
McCourt RM, Thomson DA. 1984. Cleaning behavior of the juvenile Panamic sergeant major, *Abudefduf troschel*ii (Gill), with a resume of cleaning associations in the Gulf of California and adjacent waters. California Fish Game 70:234–239.
Pearson K. 1901. On lines and planes of closest fit to systems of points in space. Philos Mag 2:559–572.
Rasband WS. 2014. ImageJ. U. S. National Institutes of Health, Bethesda, Maryland, USA. Available at: http://imagej.nih.gov/ij/, version 1.49.
Randall JE. 1986. Red Sea Reef Fishes. London: Immel Publishing. 192 p.
Randall JE, Springer VG. 1975. The monotypic Indo-Pacific labrid fish genera *Labrichthys* and *Diproctacanthus* with description of a new related genus, Larabicus. Proc Biol Soc Wash 86:279–298.
Tedman RA. 1980a. Comparative study of the cranial morphology of the labrids *Choerodon venustus* and *Labroides dimidiatus* and the scarid *Scarus fasciatus* (Pisces: Perciformes) I. Head skeleton. Aust J Mar Freshwater Res 31:337–49.
Tedman RA. 1980b. Comparative study of the cranial morphology of the labrids *Choerodon venustus* and *Labroides dimidiatus* and the scarid *Scarus fasciatus* (Pisces: Perciformes) II. Cranial myology and feeding mechanisms. Aust J Mar Freshwater Res 31:351–72.
Wainwright PC, Bellwood DR, Westneat MW, Grubich JR, Hoey AS. 2004. A functional morphospace for the skull of labrid fishes: Patterns of diversity in a complex biomechanical system. Bio J Linn Soc Lond 82:1–25.
Westneat MW. 1990. Feeding mechanics of teleost fishes (Labridae; Perciformes): A test of four-bar linkage models. J Morphol 205:269–295.
Westneat MW. 1994. Transmission of force and velocity in the feeding mechanisms of labrid fishes (Teleostei, Perciformes). Zoomorphology 114:103–118.
Winterbottom R. 1974. A descriptive synonymy of the striated muscles of the Teleostei. Proc Acad Natl Sci Phila 125:225–317.